available at www.sciencedirect.com

SCIENCE DIRECT®

journal homepage: www.elsevier.com/locate/biochempharm

Catalytic roles of CYP2D6.10 and CYP2D6.36 enzymes in mexiletine metabolism: In vitro functional analysis of recombinant proteins expressed in *Saccharomyces cerevisiae*

Nobumitsu Hanioka [a], *Yoshihito Okumura* [a], *Yoshiro Saito* [b,c], *Hiroyuki Hichiya* [b], *Akiko Soyama* [b], *Keita Saito* [a], *Kazuyuki Ueno* [d], *Jun-ichi Sawada* [b,c], *Shizuo Narimatsu* [a,*]

[a] *Graduate School of Medicine, Dentistry and Pharmaceutical Sciences, Okayama University, 1-1-1 Tsushima-naka, Okayama 700-8530, Japan*

[b] *Project Team for Pharmacogenetics, National Institute of Health Sciences, 1-18-1 Kamiyoga, Setagaya-ku, Tokyo 158-8501, Japan*

[c] *Division of Biochemistry and Immunochemistry, National Institute of Health Sciences, 1-18-1 Kamiyoga, Setagaya-ku, Tokyo 158-8501, Japan*

[d] *Department of Pharmaceutical Sciences, Niigata University of Pharmacy and Applied Life Sciences, 5-13-2 Kamishin'ei-cho, Niigata 950-2081, Japan*

ARTICLE INFO

Article history:
Received 18 January 2006
Accepted 31 January 2006

Keywords:
Mexiletine
CYP2D6
Genetic polymorphism
CYP2D6*10
CYP2D6*36

Abbreviations:
CYP, cytochrome P450
HPLC, high-performance liquid chromatography
SRS, substrate recognition site

ABSTRACT

Cytochrome P450 2D6 (CYP2D6) metabolizes approximately one-third of the medicines in current clinical use and exhibits genetic polymorphism with interindividual differences in metabolic activity. To precisely investigate the effect of *CYP2D6*10B* and *CYP2D6*36* frequently found in Oriental populations on mexiletine metabolism in vitro, CYP2D6 proteins of wild-type (CYP2D6.1) and variants (CYP2D6.10 and CYP2D6.36) were heterologously expressed in yeast cells and their mexiletine *p*- and 2-methyl hydroxylation activities were determined. Both variant CYP2D6 enzymes showed a drastic reduction of CYP2D6 holo- and apoproteins compared with those of CYP2D6.1. Mexiletine *p*- and 2-methyl hydroxylation activities on the basis of the microsomal protein level at the single substrate concentration (100 μM) of variant CYP2D6s were less than 6% for CYP2D6.10 and 1% for CYP2D6.36 of those of CYP2D6.1. Kinetic analysis for mexiletine hydroxylation revealed that the affinity toward mexiletine of CYP2D6.10 and CYP2D6.36 was reduced by amino acid substitutions. The V_{max} and V_{max}/K_m values of CYP2D6.10 on the basis of the microsomal protein level were reduced to less than 10% of those of CYP2D6.1, whereas the values on the basis of functional CYP2D6 level were comparable to those of CYP2D6.1. Although it was impossible to estimate the kinetic parameters for the mexiletine hydroxylation of CYP2D6.36, the metabolic ability toward mexiletine was considered to be poorer not only than that of CYP2D6.1 but also than that of CYP2D6.10. The same tendency was also observed in kinetic analysis for bufuralol 1″-hydroxylation as a representative CYP2D6 probe. These findings suggest that *CYP2D6*36* has a more drastic impact on mexiletine metabolism than *CYP2D6*10*.

* Corresponding author. Tel.: +81 86 251 7942; fax: +81 86 251 7942.
E-mail address: shizuo@pharm.okayama-u.ac.jp (S. Narimatsu).

0006-2952/$ – see front matter © 2006 Elsevier Inc. All rights reserved.
doi:10.1016/j.bcp.2006.01.019

1. Introduction

Mexiletine is a class 1B antiarrhythmic agent used to control ventricular arrhythmia [1]. Numerous studies have shown that there is marked interindividual variability in mexiletine plasma concentrations after a given dose [2]. As mexiletine has a narrow therapeutic index with effective and minimally toxic concentrations, monitoring the plasma concentration is desirable to ensure efficacy and to reduce the adverse effects of the drug [1,2]. Mexiletine is eliminated by both renal excretion of the unchanged compounds and extensive metabolism in humans, and less than 10% of the dose is recovered unchanged in urine [2]. The major metabolic pathways of mexiletine are aromatic hydroxylation forming *p*-hydroxymexiletine and aliphatic hydroxylation forming 2-hydroxymexiletine, which are catalyzed by hepatic cytochrome P450 (CYP) enzymes [2,3]. These metabolites have no significant antiarrhythmic activity [1,4]. Several in vivo and in vitro studies have suggested that the oxidative conversions of mexiletine to *p*- and 2-hydroxymexiletine are predominantly catalyzed by CYP2D6 in humans [5,6] (Fig. 1). It has been reported that mexiletine clearance correlates with debrisoquine 4-hydroxylation activity (poor metabolizer or extensive metabolizer), and that quinidine (a selective inhibitor of CYP2D6) decreases the clearance of mexiletine only in extensive metabolizers [6].

There are more than 50 different alleles or haplotypes of *CYP2D6* associated with deficient, decreased or increased activity of the enzyme (http://www.imm.ki.se/CYPalleles/cyp2d6.htm). The frequency of poor metabolizers, reflecting *CYP2D6*3*, *CYP2D6*4* and *CYP2D6*5*, was 5–10% in European populations and less than 1% in Oriental populations [7,8]. On the other hand, the *CYP2D6*10* allele is widely present in Oriental populations [9–11]. It has been found that Chinese intermediate metabolizers frequently carry a haplotype, characterized by *Xba*I 44 kb *CYP2D* fragments, associated with a poor metabolizer phenotype among Caucasians [12,13]. Johansson et al. [9] reported that the Chinese *Xba*I 44 kb haplotype is different from the Caucasian homologue and contains two variant CYP2D6 genes, namely $CYP2D6Ch_1$ (*CYP2D6*10B*) and $CYP2D6Ch_2$ (*CYP2D6*36*), respectively. *CYP2D6*10B*, with mutations yielding two amino acid substitutions (Pro34Ser and Ser486Thr), is the most common in the Chinese population. *CYP2D6*36* is the product of a gene conversion in exon 9 between *CYP2D7P* (pseudogene) and *CYP2D6*10B*, and causes eight amino acid substitutions (Pro34Ser, Pro469Ala, Thr470Ala, His478Ser, Gly479Arg, Phe481Val, Ala482Ser and Ser486Thr) in the C-terminal region. The allele frequency of *CYP2D6*36* in the Chinese population (37%) was 73% compared to that of *CYP2D6*10* (51%) and existed tandemly as CYP2D6*36–CYP2D6*10, a 44 kb fragment produced by the *Xba*I digestion of genomic DNA [9].

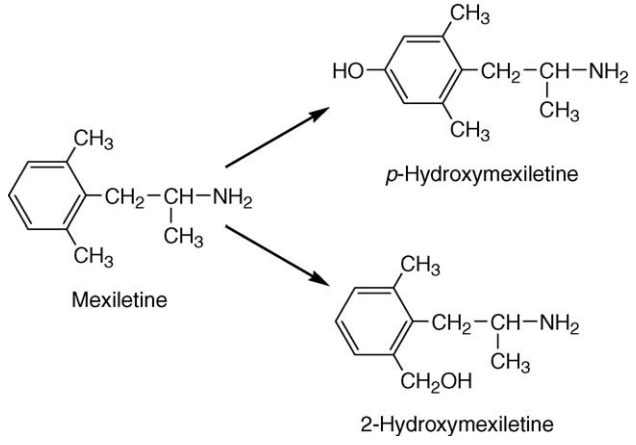

Fig. 1 – Primary metabolic pathways of mexiletine in humans.

The importance of the *CYP2D6*10* allele in the pharmacokinetics of CYP2D6 substrates in Chinese, Korean and Japanese subjects has been demonstrated [14–17]. In brief, the AUC in homozygotes for *CYP2D6*10* was reported to be approximately 2- to 5-fold higher than that in homozygotes for *CYP2D6*1* in studies with propranolol, metoprolol, proxetine and venlafaxine. A recent pharmacokinetic study demonstrated that homozygotes for *CYP2D6*10* have significantly increased plasma levels of mexiletine, although to a lesser extent, as shown in heterozygotes for *CYP2D6*5* and *CYP2D6*10* [18]. Furthermore, an in vitro study using human liver microsomes from Japanese subjects of known genotypes has suggested that the metabolism of mexiletine to *p*- and 2-hydroxymexiletine is significantly impaired in subjects with *CYP2D6*1/*10* and *CYP2D6*10/*10*, as compared with *CYP2D6*1/*1* [19]. Thus, the *CYP2D6*10* allele plays an important role in mexiletine disposition. As described above, the *CYP2D6*36* gene is closely associated with *CYP2D6*10B*, and the allele frequency of *CYP2D6*36* in the Chinese population was comparable to that of *CYP2D6*10* [9]; however, there has been no report on the detailed functions of enzyme proteins on *CYP2D6*10B* and *CYP2D6*36* mexiletine frequently detected in Oriental populations.

The purpose of this study was to precisely identify the effect of *CYP2D6*10B* and *CYP2D6*36* on mexiletine metabolism. To achieve this, the CYP2D6 proteins of wild-type (CYP2D6.1) and two variants (CYP2D6.10 and CYP2D.36) were heterologously expressed in yeast cells, and the kinetics of mexiletine *p*- and 2-methyl hydroxylation were determined.

2. Materials and methods

2.1. Materials

Human liver Quick-Clone cDNA was purchased from BD Biosciences Clontech (Mountain View, CA, USA), pENTR/D-TOPO vector was from Invitrogen (Carlsbad, CA, USA), and the QuikChange multi site-directed mutagenesis kit was from Stratagene (La Jolla, CA, USA). The expression vector pGYR1, which has a GAPDH promoter and includes the yeast NADPH-P450 reductase gene [20], was kindly provided by Dr. Yoshihiko Funae of Osaka City University (Osaka, Japan). Mexiletine was purchased from Sigma–Aldrich (St. Louis, MO, USA). Hydroxylated metabolites of mexiletine (*p*- and 2-hydroxymexiletine) were supplied by Nippon Boehringer Ingelheim (Hyogo, Japan). Bufuralol and 1″-hydroxybufuralol as hydroxychlorides were obtained from Ultrafine Chemicals (Manchester, UK), NADPH, glucose 6-phosphate and glucose 6-phosphate dehydrogenase were from Oriental Yeast (Tokyo, Japan), the BigDye terminator cycle sequencing reaction kit v3.1 was from Applied Biosystems (Foster City, CA, USA), mouse anti-CYP2D6 monoclonal

antibody was from BD Biosciences Discovery Labware (Bedford, MA, USA), and horseradish peroxidase-conjugated sheep anti-mouse immunoglobulin and enhanced chemiluminescence-plus reagents were from Amersham Biosciences (Piscataway, NJ, USA). All other chemicals and reagents used were of the highest quality commercially available.

2.2. Construction of CYP2D6 plasmids

CYP2D6*1A cDNA was cloned into the pENTR/D-TOPO vector with human liver Quick-Clone cDNA. The cDNAs of CYP2D6*10B and CYP2D6*36 were constructed with a QuikChange multi site-directed mutagenesis kit according to the manufacturer's instructions using the 5′-phosphorylated primers listed in Table 1. Mutations for CYP2D6*10B (100C > T, 336C > T, 408G > C and 1457G > C) were introduced using CYP2D6*1A in pENTR/D-TOPO as a template by one step. Mutations for CYP2D6*36 were successively introduced using CYP2D6*1A in pENTR/D-TOPO as a first template by four steps (100C > T, 1441T > G, 1443T > C and 1444G > A; 336C > T, 1445C > G, 1446T > C and 1449C > T; 408G > C, 1432C > T, 1433A > C and 1435G > C; and 1401G > C, 1405C > G, 1408A > G, 1410T > C and 1457G > C). The nucleic acid changes of 336C > T, 408G > C and 1401G > C are silent mutations encoding Phe112, Val136 and Ser467 of CYP2D6 protein, respectively. All CYP2D6 plasmids were sequenced to confirm successful mutagenesis. Each full length insert with the *Hin*dIII site in 5′- and 3′-ends encoding CYP2D6 was amplified by polymerase chain reaction (PCR), and subcloned into the pGYR1 yeast expression vector as described previously [20].

2.3. Expression of CYP2D6 enzymes

pGYR1 vectors containing CYP2D6 cDNAs were used to transform *Saccharomyces cerevisiae* AH22 by the lithium acetate method, and yeast transformants were cultivated [21]. Microsomes from yeast cells were prepared as described previously [22].

2.4. Assay for CYP2D6 holo- and apoproteins

Microsomal fractions were diluted to a protein concentration of 10 mg/ml with 100 mM potassium phosphate buffer (pH 7.4) containing 20% (v/v) glycerol and 0.4% (w/v) Emulgen 911, and total functional CYP2D6 protein levels were spectrophotometrically measured as reduced carbon monoxide (CO) spectra according to the method of Omura and Sato [23] using 91 mM^{-1} cm^{-1} as an absorption coefficient. Total CYP2D6 protein levels of holo- and apoforms in yeast cell microsomes were determined by immunoblotting as described previously with minor modifications [22]. The microsomal fractions (5.0 μg protein) were separated by 10% sodium dodecyl sulfate-polyacrylamide gel electrophoresis and electrotransferred to a polyvinylidene difluoride membrane. The membrane was incubated with mouse anti-CYP2D6 monoclonal antibody (diluted at 1:1000) as the primary antibody and with horseradish peroxidase-conjugated sheep anti-mouse immunoglobulin (diluted at 1:5000) as the secondary antibody. Immunoreactive proteins were visualized with chemifluorescence (enhanced chemiluminescence-plus reagents), and the band densities were relatively determined with Scion Image v4.0 (Scion Corporation, Frederick, MD, USA). Human liver microsomes (H161, BD Biosciences Discovery Labware) were used as a positive control.

2.5. Assay for mexiletine hydroxylation

Mexiletine hydroxylation activities were determined by measuring the formation of *p*- and 2-hydroxymexiletine, according to the method of Nakajima et al. [24] with some modifications. The incubation mixture contained mexiletine as a substrate (2–200 μM), microsomes from yeast cells (2 mg protein/ml for CYP2D6.1, 3 mg protein/ml for CYP2D6.10 and 6 mg protein/ml for CYP2D6.36), 1 mM NADPH, 10 mM glucose 6-phosphate, 1 unit/ml glucose 6-phosphate dehydrogenase and 10 mM $MgCl_2$ in 50 mM potassium phosphate buffer (pH 7.4) in a final volume of 200 μl. Mexiletine was dissolved in methanol (final concentration in the reaction medium, 0.5% (v/v)). After preincubation at 37 °C for 1 min, the reaction was started by the addition of microsomes from yeast cells. The mixture was incubated at 37 °C for 20 min and stopped with 10 μl of 2 M phosphoric acid with vortexing. The samples were centrifuged at 12,000 × *g* for 10 min at 4 °C. The supernatant was filtered with a 0.2 μm polytetra-fluoroethylene membrane filter (Millipore, Bedford, MA, USA), and a 50 μl portion was subjected to high-performance liquid chromatography (HPLC).

Table 1 – Primers used for site-directed mutagenesis

Mutation	Primer sequence	Position
100C > T[a]	5′-CTGCACGCTAC**T**CACCAGGCCCC-3′	89–111
336C > T[a]	5′-CCCAGATCCTGGGTTT**T**GGGCCGCGTTCCCAAG-3′	320–352
408G > C[a]	5′-CGCTTCTCCGT**C**TCCACCTTGCG-3′	397–419
1457G > C[b]	5′-CTTTGCTTTCCTGGTGA**C**CCCATCCCCCTATGAGC-3′	1440–1474
1401G > C; 1405C > G; 1408A > G; 1410T > C[c]	5′-CTTCAGCTTCTC**C**GTG**G**CC**G**C**C**GGACAGCCCCG-3′	1389–1421
1432C > T; 1433A > C; 1435G > C[c]	5′-CGGCCCAGCCAC**TC**T**C**GTGTCGTCAGC-3′	1420–1446
1441T > G; 1443T > C; 1444G > A[c]	5′-CAGCCACCATGGTGTC**G**T**CA**CTTTCCTGGTGAGCC-3′	1425–1459
1445C > G; 1446T > C; 1449C > T[c]	5′-CCACCATGGTGTCGTCA**GC**TT**T**CTGGTGAGCCCATCCCC-3′	1428–1466
1457G > C[c]	5′-CGTCAGCTTTCTGGTGA**C**CCCATCCCCCTATGAGC-3′	

All primers were 5′-phosphorylated. Bold and underlined letters indicate the mutation sites introduced by PCR-based mutagenesis.
[a] Primer for CYP2D6*10B and CYP2D6*36.
[b] Primer for CYP2D6*10B.
[c] Primer for CYP2D6*36.

The HPLC system consisted of an AS-8021 autosampler (Tosoh, Tokyo, Japan), a DP-8020 pump (Tosoh), a CO-8020 column oven (Tosoh), an L-7485 fluorescence detector (Hitachi, Tokyo, Japan), and a GT-102 degasser (Lab-Quatec, Tokyo, Japan) equipped with an Inertsil ODS-80A column (4.6 mm i.d. × 150 mm; GL Sciences, Tokyo, Japan). The column was maintained at 40 °C. Data acquisition was accomplished using LC-8020 v1.3 software (Tosoh). Elution was performed isocratically with 20 mM potassium phosphate containing 20 mM triethylamine (pH 2.5)-methanol (82:18, v/v) at a flow rate of 1.0 ml/min. The pH of the aqueous portion was adjusted to 2.5 with 10 M phosphoric acid. Detection was based on fluorescence intensity with excitation at 270 nm and emission at 312 nm. Standard samples were prepared in the same manner as incubation samples. Under these conditions, the retention times of *p*- and 2-hydroxymexiletine and mexiletine were 4.5, 8.3 and 31.2 min, respectively. The detection limits for *p*- and 2-hydroxymexyletine were 5.0 and 50 pmol/assay with a signal-to-noise ratio of 3, respectively. The intra- and inter-day variation coefficients did not exceed 10% in any assay.

2.6. Other methods

Protein concentrations of microsomal fractions were determined by the method of Lowry et al. [25] using bovine serum albumin as a standard. Bufuralol 1″-hydroxylation was determined as described previously [26]. The substrate and microsomal protein concentrations used for each CYP2D6 enzyme were as follows: CYP2D6.1, 0.2–20 μM and 0.1 mg protein/ml; CYP2D6.10, 0.5–50 μM and 0.5 mg protein/ml and CYP2D6.36, 2–200 μM and 2 mg protein/ml.

2.7. Data analysis

Kinetic parameters such as K_m and V_{max} for mexiletine hydroxylation and bufuralol 1″-hydroxylation were estimated by analyzing Michaelis–Menten plots or Eadie–Hofstee plots using Prism v4.0 software (GraphPad Software, San Diego, CA, USA). Intrinsic clearance values were determined as the ratio V_{max}/K_m. All values are expressed as the mean ± S.E.M. of three independent transfection experiments. Statistical comparisons were made with Student's *t*-test, and differences were considered statistically significant when the *p*-value was <0.05.

3. Results

3.1. Expression of wild-type and variant CYP2D6s in yeast cells

The expression levels of CYP2D6 proteins in microsomal fractions obtained from yeast cells transfected with CYP2D6*1A, CYP2D6*10B and CYP2D6*36 were examined by reduced CO-difference spectral and immunoblot analyses. As shown in Fig. 2A, the reduced CO-difference spectrum of CYP2D6.1 showed a large Soret peak at around 450 nm, whereas Soret peaks of CYP2D6.10 and CYP2D6.36 were much lower than that of CYP2D6.1. The functional CYP level of CYP2D6.1 was 41 pmol/mg of microsomal protein. The functional CYP levels of CYP2D6.10 and CYP2D6.36 were 6.1 and 3.7% that of CYP2D6.1, respectively (Fig. 2B). The expression levels of wild-type and variant CYP2D6 proteins in yeast cell microsomes were also assessed by immunoblotting which recognized both holo- and apoforms. The stained bands of CYP2D6.10 and CYP2D6.36 were smaller than that of CYP2D6.1, although all CYP2D6 proteins were recognized with an antibody against CYP2D6 (Fig. 3A). The expression levels of CYP2D6.10 and CYP2D6.36 were 30 and 33% that of CYP2D6.1, respectively. These differences in the levels of recombinant protein within yeast cells were reproducible in three independent transfection experiments.

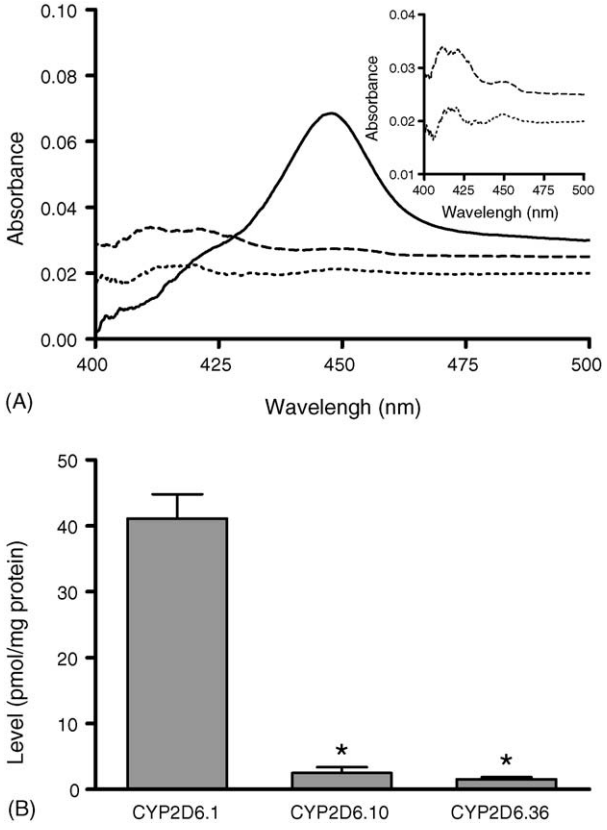

Fig. 2 – Reduced CO-difference spectra of microsomes from yeast cells expressing wild-type and variant CYP2D6s. (A) Representative results of pooled microsomes from three independent preparations. The microsomal protein concentration used was 10 mg/ml. Solid line, CYP2D6.1; broken line, CYP2D6.10; dotted line, CYP2D6.36. (B) Expression level of CYP2D6 holoprotein. The results are expressed as pmol/mg protein. Each bar represents the mean ± S.E.M. of three separate experiments derived from independent preparations. (*) Significantly different from CYP2D6.1 ($p < 0.05$).

3.2. Mexiletine hydroxylation activities of wild-type and variant CYP2D6s expressed in yeast cells

The mexiletine hydroxylation activities of CYP2D6.1, CYP2D6.10 and CYP2D6.36 were then examined. Figs. 4 and 5 show activities on the basis of microsomal and CYP2D6 protein levels at a single substrate concentration (100 μM),

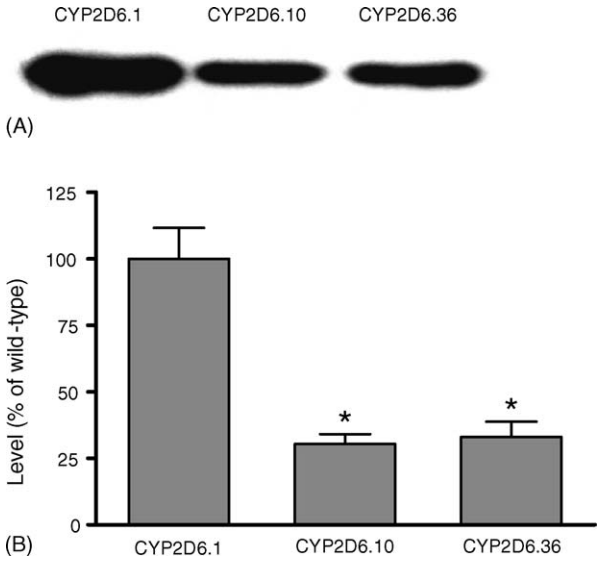

Fig. 3 – Immunoblotting of microsomes from yeast cells expressing wild-type and variant CYP2D6s. (A) Representative results of pooled microsomes from three independent preparations. The microsomal protein level applied was 5.0 μg/lane. (B) Expression level of CYP2D6 holo- and apoprotein. The results are expressed as a percentage of the CYP2D6.1 level. Each bar represents the mean ± S.E.M. of three separate experiments derived from independent preparations. (*) Significantly different from CYP2D6.1 ($p < 0.05$).

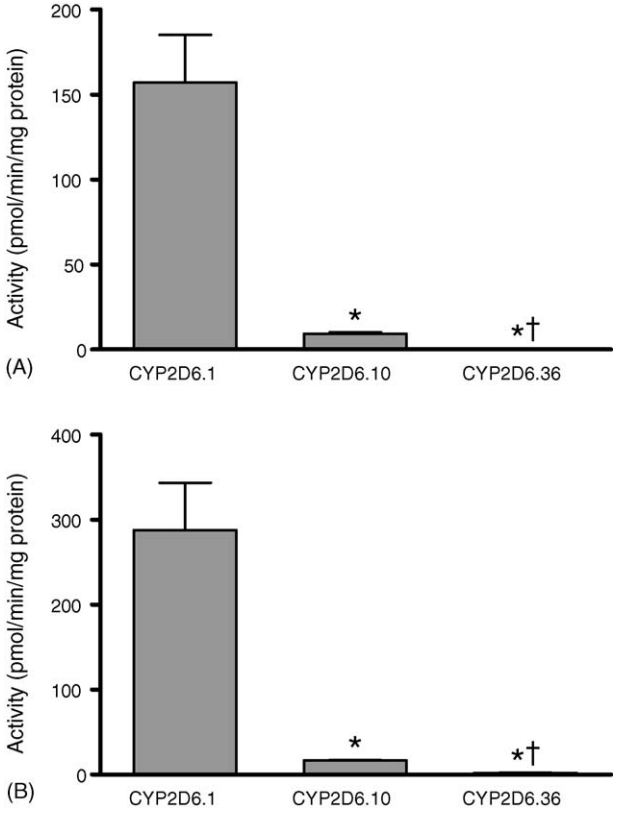

Fig. 4 – Mexiletine hydroxylation activities in microsomes from yeast cells expressing wild-type and variant CYP2D6s. (A) Mexiletine *p*-hydroxylation. (B) Mexiletine 2-methyl hydroxylation. The substrate concentration used was 100 μM. Enzyme activities are expressed as pmol/min/mg protein. Each bar represents the mean ± S.E.M. of three separate experiments derived from independent preparations. (*) Significantly different from CYP2D6.1 ($p < 0.05$). (†) Significantly different from CYP2D6.10 ($p < 0.05$).

respectively. The catalytic activities toward mexiletine of CYP2D6.1 on the basis of microsomal protein level were 160 pmol/min/mg protein for *p*-hydroxylation and 290 pmol/min/mg protein for 2-methyl hydroxylation. The activities of CYP2D6.10 and CYP2D6.36 were reduced to 5.8–5.9 and 0.3–0.6% of those of CYP2D6.1, respectively. The formation of *p*- and 2-hydroxylmexiletine was not detectable in CYP2D6.36 at lower substrate concentrations (<50 μM). On the other hand, mexiletine *p*- and 2-methyl hydroxylation activities of CYP2D6.1 on the basis of the CYP2D6 level were 3.9 and 7.1 pmol/min/pmol CYP2D6, respectively. In both hydroxylation reactions, the activities of CYP2D6.10 were comparable to those of CYP2D6.1, whereas the activities of CYP2D6.36 were 10–23% of those of CYP2D6.1.

To obtain further information on the metabolic ability of variant CYP2D6s as well as wild-type CYP2D6 toward mexiletine, kinetic analyses for mexiletine *p*- and 2-methyl hydroxylation were performed. The nonlinear regression curves of Michaelis–Menten kinetics are shown in Fig. 6. The kinetic parameters of CYP2D6.36 could not be accurately established using HPLC analysis due to low activity in any mexiletine hydroxylation. As summarized in Table 2, the K_m values for mexiletine *p*- and 2-methyl hydroxylation of CYP2D6.1 were 14 and 13 μM, respectively. The K_m value for mexiletine *p*-hydroxylation of CYP2D6.10 was significantly higher (1.7-fold) than that of CYP2D6.1, whereas no significant difference was observed in the K_m values of CYP2D6.1 and CYP2D6.10 for 2-methyl hydroxylation. The V_{max} and V_{max}/K_m values for mexiletine hydroxylation of CYP2D6.1 on the basis of microsomal protein level were 180 pmol/min/mg protein and 13 μl/min/mg protein for *p*-hydroxylation, and 320 pmol/min/mg protein and 24 μl/min/mg protein for 2-methyl hydroxylation, respectively. The V_{max} values for mexiletine *p*- and 2-methyl hydroxylation of CYP2D6.10 were 6.2–6.7% of those of CYP2D6.1, and the V_{max}/K_m values were reduced to less than 5% of CYP2D6.1. When the activities were normalized to functional CYP2D6 holoprotein levels, the V_{max} and V_{max}/K_m values for mexiletine hydroxylation of CYP2D6.1 were 4.4 pmol/min/pmol CYP2D6 and 0.32 μl/min/pmol CYP2D6 for *p*-hydroxylation, and 8.0 pmol/min/pmol CYP2D6 and 0.60 μl/min/pmol CYP2D6 for 2-methyl hydroxylation, respectively. Therefore, the V_{max} and V_{max}/K_m values for mexiletine *p*- and 2-methyl hydroxylation were comparable between CYP2D6.1 and CYP2D6.10.

3.3. *Bufuralol 1″-hydroxylation activities of wild-type and variant CYP2D6s expressed in yeast cells*

The bufuralol 1″-hydroxylation activities as a representative CYP2D6 probe of wild-type and variant CYP2D6 enzymes were

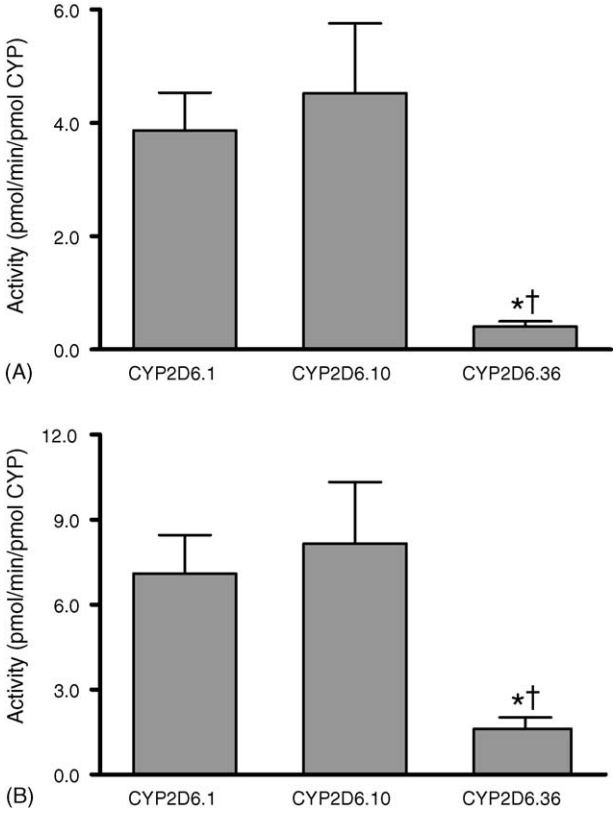

Fig. 5 – Mexiletine hydroxylation activities in microsomes from yeast cells expressing wild-type and variant CYP2D6s. (A) Mexiletine *p*-hydroxylation. (B) Mexiletine 2-methyl hydroxylation. The substrate concentration used was 100 μM. The results are expressed as pmol/min/pmol CYP2D6. Each bar represents the mean ± S.E.M. of three separate experiments derived from independent preparations. (*) Significantly different from CYP2D6.1 ($p < 0.05$). (†) Significantly different from CYP2D6.10 ($p < 0.05$).

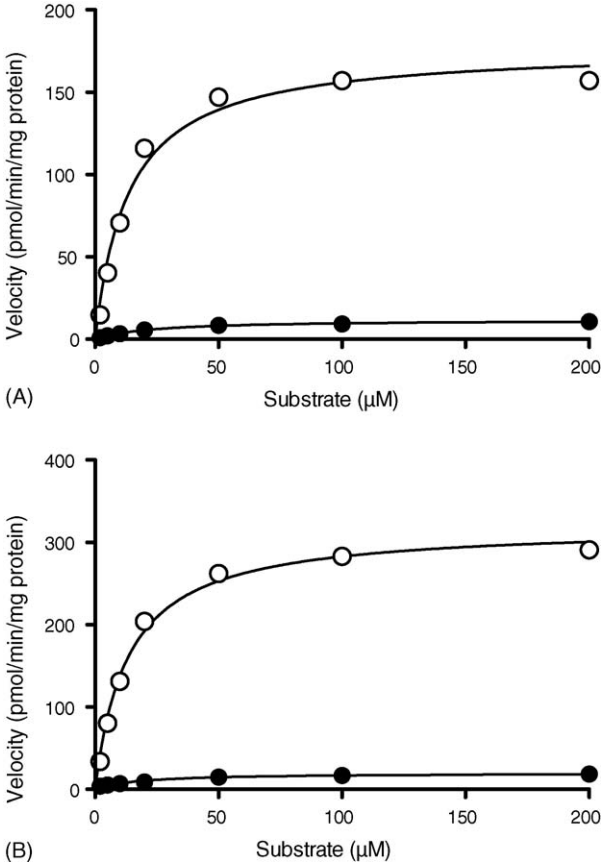

Fig. 6 – Michaelis–Menten kinetics for mexiletine hydroxylation by microsomes from yeast cells expressing wild-type and variant CYP2D6s. (A) Mexiletine *p*-hydroxylation. (B) Mexiletine 2-methyl hydroxylation. The substrate concentrations used were 2–200 μM. The results are expressed as pmol/min/mg protein. Each point represents the mean of three separate experiments derived from independent preparations. Open circle, CYP2D6.1; closed circle, CYP2D6.10.

also determined. The activities were measured at seven different substrate concentrations, and nonlinear regression curves of the Michaelis–Menten equation were designed. The calculated kinetic parameters are summarized in Table 3. The K_m value of CYP2D6.1 was 2.4 μM, and the values of CYP2D6.10 and CYP2D6.36 were significantly higher (2.7- and 13-fold, respectively) than that of CYP2D6.1. The V_{max} and V_{max}/K_m values of CYP2D6.1 on the basis of microsomal protein levels were 2300 pmol/min/mg protein and 950 μl/min/mg protein, respectively, and a remarkable reduction in CYP2D6.10 and CYP2D6.36 was observed. The V_{max} values of CYP2D6.10 and CYP2D6.36 were 13 and 2.1% that of CYP2D6.1, respectively. As for V_{max}/K_m, the values of CYP2D6.10 and CYP2D6.36 were 5.0 and 0.17% that of CYP2D6.1, respectively. Furthermore, the V_{max} and V_{max}/K_m values for bufuralol 1″-hydroxylation were normalized to functional CYP2D6 holoprotein levels to assess the intrinsic function of wild-type and variant CYP2D6 enzymes. The V_{max} and V_{max}/K_m values of CYP2D6.1 were 57 pmol/min/pmol CYP2D6 and 24 μl/min/pmol CYP2D6, respectively. There was no significant difference in V_{max} and V_{max}/K_m values between CYP2D6.1 and CYP2D6.10. In contrast, the V_{max} and V_{max}/K_m values of CYP2D6.36 were reduced to 62 and 4.6% of CYP2D6.1, respectively.

4. Discussion

Mexiletine is a widely prescribed antiarrhythmic agent, and its therapeutic index is narrow because of marked interindividual variability in mexiletine clearance [1,2]. Previous reports have suggested that CYP2D6 plays an important clinical role in the metabolism of mexiletine [5,6]. Since the *CYP2D6* gene is highly polymorphic and shows marked interethnic differences (http://www.imm.ki.se/CYPalleles/cyp2d6.htm), it is important to clarify its effect on the metabolism of mexiletine for individual drug therapy. In this study, we focused on the two *CYP2D6* alleles, *CYP2D6*10B* and *CYP2D6*36*, widely found in the Japanese population, and investigated mexiletine *p*- and 2-methyl hydroxylation in microsomes from yeast cells expressing wild-type and variant CYP2D6s.

Table 2 – Kinetic parameters for mexiletine hydroxylation by microsomes from yeast cells expressing wild-type and variant CYP2D6s

	K_m[a]	V_{max}		V_{max}/K_m	
		Protein[b]	CYP[c]	Protein[d]	CYP[e]
p-Hydroxylation					
CYP2D6.1	13.5 ± 0.5	177 ± 34	4.36 ± 0.80	13.0 ± 2.4	0.32 ± 0.05
CYP2D6.10	23.1 ± 2.0*	11.8 ± 1.4*	5.72 ± 1.56	0.51 ± 0.03*	0.25 ± 0.07
CYP2D6.36		<0.10	<0.01		
2-Methyl hydroxylation					
CYP2D6.1	13.0 ± 1.9	323 ± 69	7.98 ± 1.68	24.4 ± 1.8	0.60 ± 0.07
CYP2D6.10	18.4 ± 3.9	19.9 ± 1.6*	9.62 ± 2.49	1.14 ± 0.14*	0.56 ± 0.19
CYP2D6.36		<2.00	<0.20		

Each value represents the mean ± S.E.M. of three separate experiments derived from independent preparations.
[a] μM.
[b] pmol/min/mg protein.
[c] pmol/min/pmol CYP2D6.
[d] μl/min/mg protein.
[e] μl/min/pmol CYP2D6.
* Significantly different from CYP2D6.1 ($p < 0.05$).

The expression of CYP2D6 protein was confirmed by immunoblotting. Furthermore, 450 nm absorbance was measured by reduced CO-difference spectra in yeast cell microsomal fractions. The CYP2D6 protein levels of CYP2D6.10 and CYP2D6.36 were markedly low compared with that of CYP2D6.1. The contents of functional CYP2D6 holoproteins in CYP2D6.10 and CYP2D6.36 estimated by reduced CO-difference spectra were much lower than those calculated on staining intensities of protein bands immunoreacted with the CYP2D6 antibody. Previous studies have also found that the substitution of Pro34Ser but not Ser486Thr decreased the expression level of CYP2D6 protein, suggesting that the reduction in mutant CYP2D6 proteins with Pro34Ser has a relatively low capability in anchoring into the membrane of endoplasmic reticulum of yeast cells [9,27,28]. The profile of CYP2D6 protein levels obtained in this study agreed with other reports. Therefore, it is reasonable to think that low protein levels of CYP2D6.36 may be mainly attributable to the substitution of Pro34Ser but not Pro469Ala, Thr470Ala, His478Ser, Gly479Arg, Phe481Val, Ala482Ser or Ser486Thr, because the levels of CYP2D6.10 and CYP2D6.36 proteins were much the same in both immunoblots and reduced CO-difference spectral analyses.

Nakajima et al. [24] estimated by the relative activity factor that the contribution of CYP2D6 to mexiletine hydroxylation is 60–98%, suggesting the importance of CYP2D6 in mexiletine metabolism. Therefore, we examined the effect of *CYP2D6*10B* and *CYP2D6*36* on mexiletine hydroxylation using recombinant CYP2D6 enzymes expressed in yeast cells. Additionally, bufuralol 1″-hydroxylation activity was also determined to characterize the enzymatic function of variant CYP2D6 enzymes toward a typical CYP2D6 substrate. The enzymatic activities in this study were analyzed in two ways: as pmol/min/mg protein (on the basis of microsomal protein level), and as pmol/min/pmol CYP2D6 (on the basis of functional CYP2D6 level). CYP2D6.10, with Pro34Ser and Ser486Thr substitutions, was capable of catalyzing mexiletine *p*- and 2-methyl hydroxylation comparable to wild-type CYP2D6.1 at the substrate concentrations examined; however, the capability of CYP2D6.10 to hydroxylate mexiletine on the basis of the microsomal protein level was much lower than that of CYP2D6.1. On the other hand, the formation of *p*- and

Table 3 – Kinetic parameters for bufuralol 1″-hydroxylation by microsomes from yeast cells expressing wild-type and variant CYP2D6s

	K_m[a]	V_{max}		V_{max}/K_m	
		Protein[b]	CYP[c]	Protein[d]	CYP[e]
CYP2D6.1	2.34 ± 0.26	2340 ± 440	57.0 ± 8.9	950 ± 100	23.6 ± 3.68
CYP2D6.10	6.54 ± 0.31*	311 ± 21*	147 ± 33	47.9 ± 4.3*	22.6 ± 5.12
CYP2D6.36	31.8 ± 3.4*,†	49.8 ± 5.96*,†	35.2 ± 6.7*,†	1.58 ± 0.15*,†	1.09 ± 0.12*,†

Each value represents the mean ± S.E.M. of three separate experiments derived from independent preparations.
[a] μM.
[b] pmol/min/mg protein.
[c] pmol/min/pmol CYP2D6.
[d] μl/min/mg protein.
[e] μl/min/pmol CYP2D6.
* Significantly different from CYP2D6.1 ($p < 0.05$).
† Significantly different from CYP2D6.10 ($p < 0.05$).

2-hydroxymexiletine by CYP2D6.36 with eight substitutions (Pro34Ser, Pro469Ala, Thr470Ala, His478Ser, Gly479Arg, Phe481Val, Ala482Ser and Ser486Thr) was undetectable at lower substrate concentrations, and the metabolites generated even at high substrate concentrations were less than 1% of CYP2D6.1.

We further tried to determine the kinetic parameters for mexiletine *p*- and 2-methyl hydroxylation of wild-type and variant CYP2D6s, and confirmed that the kinetics in all CYP2D6 proteins fit the single enzyme model with a typical Michaelis–Menten equation. The K_m values for the mexiletine hydroxylation of wild-type CYP2D6 obtained in this study were almost identical to those of other studies in an expression system using human B-lymphoblastoid cells [24]. The K_m values of CYP2D6.10 were slightly higher than those of CYP2D6.1, and a significant difference was observed only for *p*-hydroxylation. Although it was impossible to calculate kinetic parameters for the mexiletine hydroxylation of CYP2D6.36 due to low analytical sensitivity, the affinity of CYP2D6.36 toward mexiletine was roughly estimated as a lower value than that of CYP2D6.10 in both hydroxylation reactions from the ratio of activity at a substrate concentration of 100 μM to that of 200 μM (data not shown). A similar tendency was observed in bufuralol 1″-hydroxylation for both variant CYP2D6s, with a K_m value ranking of CYP2D6.36 > CYP2D6.10 > CYP2D6.1, in good agreement with the previous report [27]. Therefore, we consider that the reduced affinity of CYP2D6 toward mexiletine as well as bufuralol is closely associated with Pro34 and the additional six amino acid residues substituted by the gene conversion between *CYP2D7P* and *CYP2D6*10B* in exon 9.

V_{max} and V_{max}/K_m values for the mexiletine hydroxylation of CYP2D6.10 on the basis of the microsomal protein level were reduced to less than 10% those of CYP2D6.1, whereas the kinetic parameters on the basis of functional CYP2D6 level exhibited similar values between CYP2D6.1 and CYP2D6.10. Thus, the reduced V_{max} values on the basis of microsomal protein level were attributed to the reduced holoprotein levels but not to the change in the intrinsic enzyme function. As for CYP2D6.36, the activities of both hydroxylation reactions were too low to determine the V_{max} and V_{max}/K_m values. Similarly, significant reductions of V_{max} and V_{max}/K_m values for the bufuralol 1″-hydroxylation of CYP2D6.10 were observed only in pmol/min/mg protein units. These results by CYP2D6.36 exhibited lower V_{max} and V_{max}/K_m values compared with those of CYP2D6.1 in any unit term, suggesting that the profile for the functional alteration of CYP2D6.10 and CYP2D6.36 is generally parallel between mexiletine hydroxylation and bufuralol 1″-hydroxylation.

The X-ray crystal structures of five mammalian CYP isoforms (rabbit CYP2B4 and CYP2C5, and human CYP2C8, CYP2C9 and CYP3A4) have been reported to date [29–33]. Lewis [34,35] and Venhorst et al. [36] generated homology modeling for CYP2D6 using the CYP2C5 crystal structure as a template, and identified functionally significant regions and residues. The Pro34 residue is well conserved among most of the CYP2 family, and the residue consists of a proline-rich motif (PPGPXPXPXXGN) in the N-terminal region of CYPs which plays a significant role in the proper assembly of the native enzyme [37]. Indeed, CYP2D6.10 and CYP2D6.36 allelic enzymes containing Pro34Ser substitution were poorly expressed in yeast cells compared with CYP2D6.1, and the catalytic activities toward mexiletine and bufuralol on the basis of the microsomal protein level were remarkably reduced by amino acid substitution. The Ser486 residue substituted in both CYP2D6.10 and CYP2D6.36 is not located in the proline-rich motif or substrate recognition site (SRS). In addition, previous site-directed mutagenesis studies have suggested that the single amino acid substitution of Ser486Thr is not associated with the expression efficiency and enzymatic function of CYP2D6 protein [27,28]. With regard to other amino acid residues of interest in CYP2D6.36, the His478, Gly479, Phe481, Ala482 residues of CYP2D6 are located in β4-1-, β6-2- and β4-2-sheets containing SRS6, and Phe481 has been particularly suggested as critical for interaction (π–π interaction) with the substrate [34,35]. Furthermore, Gly at position 479 is substituted to Arg, which has a basic side chain (guanidinium) in CYP2D6.36, and ionic interaction between the Arg and CYP2D6 substrate may also affect CYP2D6 functions. Pro469 and Thr470 residues of CYP2D6 lie at the end of the β3-3-sheet and only 7 and 6 amino acids upstream of SRS6 [34,36]. More recently, Rowland et al. have constructed the active site cavity of CYP2D6 on the basis of the crystal structure of CYP2D6. Additionally, they have suggested that the amino residues 468–487 are located in β sheet 4 [38]. Therefore, we consider that amino acid substitutions at the C-terminal region of CYP2D6.36 may also influence the conformation or flexibility in β-strands, causing a loss in enzymatic activity. Additional site-directed mutagenesis studies are required to clarify the reduction mechanisms of protein expression and enzymatic function in CYP2D6.36 using various mutated CYP2D6.

In conclusion, we expressed two allelic variant CYP2D6 enzymes (CYP2D6.10 and CYP2D6.36) widely found in Oriental populations as well as wild-type CYP2D6 (CYP2D6.1) in yeast cells, and examined their catalytic activities toward mexiletine. Both variant CYP2D6 enzymes showed a drastic reduction of CYP2D6 holo- and apoprotein levels compared with the wild-type. The mexiletine *p*- and 2-methyl hydroxylation activities of CYP2D6.10 on the basis of the microsomal protein level were reduced to less than 10% that of CYP2D6.1, whereas the values on the basis of the functional CYP2D6 level were comparable to those of CYP2D6.1. CYP2D6.36 activities were poorer not only than those of CYP2D6.1 but also than those of CYP2D6.10 in any unit term. These findings suggest that *CYP2D6*36* has a more drastic impact on mexiletine metabolism than *CYP2D6*10*. Since *CYP2D6*36* was suggested to be located with *CYP2D6*10B* on the human genome (*XbaI* 44 kb haplotype) at least in the Chinese population [9], our results suggested that the contribution of only *CYP2D6*10* should be considered and that of *CYP2D6*36* may be rejected for mexiletine metabolism in patients with the haplotype.

Acknowledgements

This work was supported in part by a Program for the Promotion of Fundamental Studies in Health Sciences, a grant from the Japan Health Sciences Foundation, and in part by a Grant-in-Aid from the Japan Research Foundation for Clinical Pharmacology.

REFERENCES

[1] Campbell NP, Kelly JG, Adgey AA, Shanks RG. The clinical pharmacology of mexiletine. Br J Clin Pharmacol 1978;6:103–8.
[2] Labbé L, Turgeon J. Clinical pharmacokinetics of mexiletine. Clin Pharmacokinet 1999;37:361–84.
[3] Beckett AH, Chidomere EC. The identification and analysis of mexiletine and its metabolic products in man. J Pharm Pharmacol 1977;29:281–5.
[4] Woosley RL, Wang T, Stone W, Siddoway L, Thompson K, Duff HJ, et al. Pharmacology, electrophysiology, and pharmacokinetics of mexiletine. Am Heart J 1984;107: 1058–65.
[5] Broly F, Libersa C, Lhermitte M. Mexiletine metabolism in vitro by human liver. Drug Metab Dispos 1990;18:362–8.
[6] Turgeon J, Fiset C, Giguere R, Gilbert M, Moerike K, Rouleau JR, et al. Influence of debrisoquine phenotype and of quinidine on mexiletine disposition in man. J Pharmacol Exp Ther 1991;259:789–98.
[7] Broly F, Gaedigk A, Heim M, Eichelbaum M, Morike K, Meyer UA. Debrisoquine/sparteine hydroxylation genotype and phenotype: analysis of common mutations and alleles of CYP2D6 in a European population. DNA Cell Biol 1991;10:545–58.
[8] Horai Y, Nakano M, Ishizaki T, Ishikawa K, Zhou HH, Zhou BI, et al. Metoprolol and mephenytoin oxidation polymorphisms in Far Eastern Oriental subjects: Japanese versus mainland Chinese. Clin Pharmacol Ther 1989;46:198–207.
[9] Johansson I, Oscarson M, Yue QY, Bertilsson L, Sjoqvist F, Ingelman-Sundberg M. Genetic analysis of the Chinese cytochrome P4502D locus: characterization of variant *CYP2D6* genes present in subjects with diminished capacity for debrisoquine hydroxylation. Mol Pharmacol 1994;46:452–9.
[10] Yokota H, Tamura S, Furuya H, Kimura S, Watanabe M, Kanazawa I, et al. Evidence for a new variant *CYP2D6* allele *CYP2D6J* in a Japanese population associated with lower in vivo rates of sparteine metabolism. Pharmacogenetics 1993;3:256–63.
[11] Kubota T, Yamaura Y, Ohkawa N, Hara H, Chiba K. Frequencies of *CYP2D6* mutant alleles in a normal Japanese population and metabolic activity of dextromethorphan O-demethylation in different CYP2D6 genotypes. Br J Clin Pharmacol 2000;50:31–4.
[12] Yue QY, Bertilsson L, Dahl-Puustinen ML, Säwe J, Sjöqvist F, Johansson I, et al. Disassociation between debrisoquine hydroxylation phenotype and genotype among Chinese. Lancet 1989;2:870.
[13] Johansson I, Yue QY, Dahl ML, Heim M, Säwe J, Bertilsson L, et al. Genetic analysis of the interethnic difference between Chinese and Caucasians in the polymorphic metabolism of debrisoquine and codeine. Eur J Clin Pharmacol 1991;40:553–6.
[14] Lai ML, Wang SL, Lai MD, Lin ET, Tse M, Huang JD. Propranolol disposition in Chinese subjects of different CYP2D6 genotypes. Clin Pharmacol Ther 1995;58: 264–8.
[15] Fukuda T, Yamamoto I, Nishida Y, Zhou Q, Ohno M, Takada K, et al. Effect of the *CYP2D6*10* genotype on venlafaxine pharmacokinetics in healthy adult volunteers. Br J Clin Pharmacol 1999;47:450–3.
[16] Huang J, Chuang SK, Cheng CL, Lai ML. Pharmacokinetics of metoprolol enantiomers in Chinese subjects of major *CYP2D6* genotypes. Clin Pharmacol Ther 1999;65: 402–7.
[17] Yoon YR, Cha IJ, Shon JH, Kim KA, Cha YN, Jang IJ, et al. Relationship of paroxetine disposition to metoprolol metabolic ratio and *CYP2D6*10* genotype of Korean subjects. Clin Pharmacol Ther 2000;67:567–76.
[18] Otani M, Fukuda T, Naohara M, Maune H, Senda C, Yamamoto I, et al. Impact of *CYP2D6*10* on mexiletine pharmacokinetics in healthy adult volunteers. Eur J Clin Pharmacol 2003;59:395–9.
[19] Senda C, Yamaura Y, Kobayashi K, Fujii H, Minami H, Sasaki Y, et al. Influence of the CYP2D6*10 allele on the metabolism of mexiletine by human liver microsomes. Br J Clin Pharmacol 2001;52:100–3.
[20] Sakaki T, Akiyoshi-Shibata M, Yabusaki Y, Ohkawa H. Organella-targeted expression of rat liver cytochrome P450c27 in yeast: genetically engineered alteration of mitochondrial P450 into a microsomal form creates a novel functional electron transport chain. J Biol Chem 1992;267:16497–502.
[21] Wan J, Imaoka S, Chow T, Hiroi T, Yabusaki Y, Funae Y. Expression of four rat CYP2D isoforms in *Saccharomyces cerevisiae* and their catalytic specificity. Arch Biochem Biophys 1997;348:383–90.
[22] Hichiya H, Takemi C, Tsuzuki D, Yamamoto S, Asaoka K, Suzuki S, et al. Complementary DNA cloning and characterization of cytochrome P450 2D29 from Japanese monkey liver. Biochem Pharmacol 2002;64:1101–10.
[23] Omura T, Sato R. The carbon monoxide-binding pigment of liver microsomes. I. Evidence for its hemoprotein nature. J Biol Chem 1964;239:2370–8.
[24] Nakajima M, Kobayashi K, Shimada N, Tokudome S, Yamamoto T, Kuroiwa Y. Involvement of CYP1A2 in mexiletine metabolism. Br J Clin Pharmacol 1998;46: 55–62.
[25] Lowry OH, Rosebrough NJ, Farr AL, Randall RJ. Protein measurement with the Folin phenol reagent. J Biol Chem 1951;193:265–75.
[26] Hanioka N, Ozawa S, Jinno H, Tanaka-Kagawa T, Nishimura T, Ando M, et al. Interaction of irinotecan (CPT-11) and its active metabolite 7-ethyl-10-hydroxycamptothecin (SN-38) with human cytochrome P450 enzymes. Drug Metab Dispos 2002;30:391–6.
[27] Fukuda T, Nishida Y, Imaoka S, Hiroi T, Naohara M, Funae Y, et al. The decreased in vivo clearance of CYP2D6 substrates by CYP2D6*10 might be caused not only by the low-expression but also by low affinity of CYP2D6. Arch Biochem Biophys 2000;380:303–8.
[28] Tsuzuki D, Takemi C, Yamamoto S, Tamagake K, Imaoka S, Funae Y, et al. Functional evaluation of cytochrome P450 2D6 with Gly42Arg substitution expressed in *Saccharomyces cerevisiae*. Pharmacogenetics 2001;11:709–18.
[29] Williams PA, Cosme J, Sridhar V, Johnson EF, McRee DE. Mammalian microsomal cytochrome P450 monooxygenase: structural adaptations for membrane binding and functional diversity. Mol Cell 2000;5: 121–31.
[30] Williams PA, Cosme J, Ward A, Angove HC, Vinković DM, Jhoti H. Crystal structure of human cytochrome P450 2C9 with bound warfarin. Nature 2003;424:464–8.
[31] Williams PA, Cosme J, Vinković DM, Ward A, Angove HC, Day PJ, et al. Crystal structures of human cytochrome P450 3A4 bound to metyrapone and progesterone. Science 2004;305:683–6.
[32] Schoch GA, Yano JK, Wester MR, Griffin KJ, Stout CD, Johnson EF. Structure of human microsomal cytochrome P450 2C8: evidence for a peripheral fatty acid binding site. J Biol Chem 2004;279:9497–503.
[33] Scott EE, White MA, He YA, Johnson EF, Stout CD, Halpert JR. Structure of mammalian cytochrome P450 2B4

complexed with 4-(4-chlorophenyl)imidazole at 1.9-Å resolution: insight into the range of P450 conformations and the coordination of redox partner binding. J Biol Chem 2004;279:27294–301.
[34] Lewis DF. Homology modelling of human CYP2 family enzymes based on the CYP2C5 crystal structure. Xenobiotica 2002;32:305–23.
[35] Lewis DF. Essential requirements for substrate binding affinity and selectivity toward human CYP2 family enzymes. Arch Biochem Biophys 2003;409: 32–44.
[36] Venhorst J, ter Laak AM, Commandeur JN, Funae Y, Hiroi T, Vermeulen NP. Homology modeling of rat and human cytochrome P450 2D (CYP2D) isoforms and computational rationalization of experimental ligand-binding specificities. J Med Chem 2003;46:74–86.
[37] Kemper B. Structural basis for the role in protein folding of conserved proline-rich regions in cytochromes P450. Toxicol Appl Pharmacol 2004;19:305–15.
[38] Rowland P, Blaney FE, Smyth MG, Jones JJ, Leydon VR, Oxbrow AK, et al. Crystal structure of human cytochrome P450 2D6. J Biol Chem, in press.